AD-A124 881 MORPHOLOGIC CHANGES IN RAT RETINA AFTER MASSIVE EXCHANGE TRANSFUSION WITH.. (U) LETTERMAN ARMY INST OF RESEARCH PRESIDIO OF SAN FRANCISCO CA 1/1

UNCLASSIFIED S T SCHUSCHEREBA ET AL. DEC 82 LAIR-134 F/G 6/16 NL

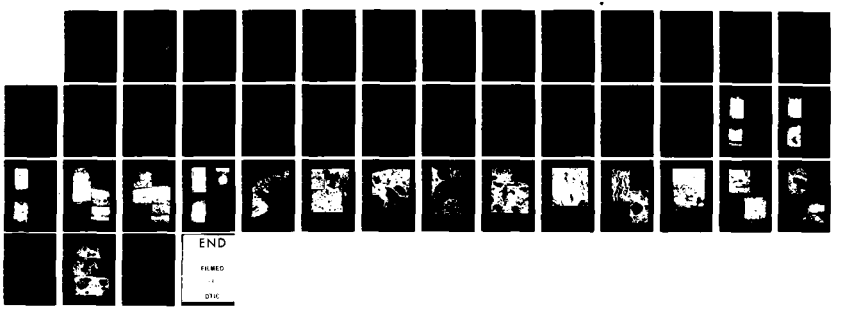

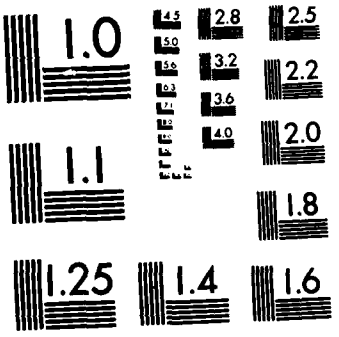

INSTITUTE REPORT NO. 134

MORPHOLOGIC CHANGES IN RAT RETINA AFTER MASSIVE EXCHANGE TRANSFUSION WITH 7% (CRYSTALLIZED) STROMA–FREE HEMOGLOBIN SOLUTION

STEVEN T. SCHUSCHEREBA, MA
HAROLD I. FRIEDMAN, MD, PhD
FRANK DeVENUTO, PhD
and
EDWIN S. BEATRICE, MD

RESEARCH SUPPORT DIVISION
BLOOD RESEARCH DIVISION
and
OCULAR HAZARDS DIVISION

DECEMBER 1982

LETTERMAN ARMY INSTITUTE OF RESEARCH
PRESIDIO OF SAN FRANCISCO, CALIFORNIA 94129

MORPHOLOGIC CHANGES IN RAT RETINA AFTER MASSIVE EXCHANGE TRANSFUSION WITH 7% (CRYSTALLIZED) STROMA–FREE HEMOGLOBIN SOLUTION--Schuschereba et al.

In conducting the research described in this report, the investigation adhered to the "Guide for the Care and Use of Laboratory Animals," as promulgated by the Committee on Revision of the Guide for Laboratory Animal Facilities and Care, Institute of Laboratory Animal Resources, National Research Council.

This material has been reviewed by Letterman Army Institute of Research and there is no objection to its presentation and/or publication. The opinions or assertions contained herein are the private views of the author(s) and are not to be construed as official or as reflecting the views of the Department of the Army or the Department of Defense. *(AR 360-5)*

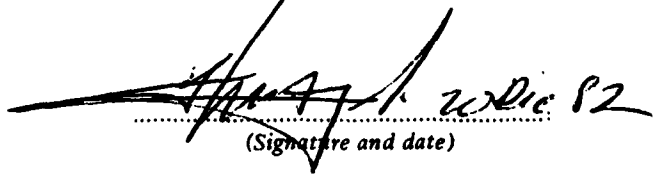

(Signature and date)

UNCLASSIFIED

SECURITY CLASSIFICATION OF THIS PAGE (When Data Entered)

REPORT DOCUMENTATION PAGE		READ INSTRUCTIONS BEFORE COMPLETING FORM
1. REPORT NUMBER Institute Report No. 134	2. GOVT ACCESSION NO. AD-A124 881	3. RECIPIENT'S CATALOG NUMBER
4. TITLE (and Subtitle) Morphologic Changes in Rat Retina After Massive Exchange Transfusion with 7% (Crystallized) Stroma-Free Hemoglobin Solution		5. TYPE OF REPORT & PERIOD COVERED Interim 1980-1981 6. PERFORMING ORG. REPORT NUMBER
7. AUTHOR(s) S.T. Schuschereba, MA; H.I. Friedman, MD, PhD; F. DeVenuto, PhD; E.S. Beatrice, MD, COL, MC		8. CONTRACT OR GRANT NUMBER(s)
9. PERFORMING ORGANIZATION NAME AND ADDRESS Divisions of Research Support, Combat Casualty Care & Blood Research, Letterman Army Institute of Research, Presidio of San Francisco, CA 94129		10. PROGRAM ELEMENT, PROJECT, TASK AREA & WORK UNIT NUMBERS Proj No. 3S162772.874-AC WU 090
11. CONTROLLING OFFICE NAME AND ADDRESS U.S. Army Medical Research and Development Command Fort Detrick Frederick, MD 21701		12. REPORT DATE December 1982 13. NUMBER OF PAGES 42
14. MONITORING AGENCY NAME & ADDRESS(if different from Controlling Office)		15. SECURITY CLASS. (of this report) UNCLASSIFIED 15a. DECLASSIFICATION/DOWNGRADING SCHEDULE

16. DISTRIBUTION STATEMENT (of this Report)

APPROVED FOR PUBLIC RELEASE; DISTRIBUTION IS UNLIMITED

17. DISTRIBUTION STATEMENT (of the abstract entered in Block 20, if different from Report)

18. SUPPLEMENTARY NOTES

19. KEY WORDS (Continue on reverse side if necessary and identify by block number)

Stroma-free hemoglobin; retinal morphology; optic disc; nerve fiber layer; ganglion cells; glycogen; transfusion; ischemia

20. ABSTRACT (Continue on reverse side if necessary and identify by block number)

Retinal morphology serves as an extremely sensitive endpoint to hypoxic and ischemic conditions manifested by circulatory pertubations. Therefore the effect of massive transfusion of stroma-free hemoglobin solution (SFHS) on retinal morphology of rats was evaluated. Seventy-three rats were divided into three groups. Two groups were transfused to 75% blood volume replacement -- one (n = 30) with 7% SFHS; one (n = 26) with 7% albumin solution; and the third group (n = 17) was cannulated, not transfused (controls). Animals in each

DD FORM 1 JAN 73 1473 EDITION OF 1 NOV 65 IS OBSOLETE

UNCLASSIFIED

SECURITY CLASSIFICATION OF THIS PAGE (When Data Entered)

20. Abstract (Cont)

group were killed at 1, 5, 12, 24 hr, and 2 mo after the procedure. In the transfused rats, focal and perivascular regions of edema, axonal swelling, and vacuoles were observed by light and transmission electron microscopy in the nerve fiber layer of the central retina. These conditions progressively decreased from 1 to 12 hr in the albumin-treated group. The retinas of SFHS-treated rats killed at 12 and 24 hr had similar but more severe morphologic changes than any of the albumin-treated animals; swelling was more severe in retinas obtained at 24 than at 12 hr, while vacuoles were larger in retinas obtained at 12 hr. Abnormalities were observed in the prelaminar portion of the optic disc of the SFHS-treated groups killed at 12 and 24 hr. Subretinal hemorrhaging occurred in about 50% of the SFHS-treated animals killed at both 12 and 24 hr and was associated with swelling, vacuolization, and disruption of the photoreceptor outer segments and retinal pigment epithelium. Below normal levels of glycogen were present in the Muller cells of the retinas of albumin-treated rats killed at 5, 12, and 24 hr. At 12 hr after transfusion the Muller cells in lesions of the retinas obtained from the SFHS-treated rats were devoid of glycogen. High glycogen levels, however, appeared in a zone peripheral to the lesions. The latter effect was not apparent in the specimens obtained at 24 hr. The damage observed was probably due to hypoxic and ischemic effects secondary to urinary hemoglobin excretion and concomitant blood volume loss. No abnormalities were seen in the controls. The retinas of SFHS-treated rats killed at 1 and 5 hr showed normal retinal morphology and glycogen levels. Presumably, SFHS exerted a protective effect during this time period. If the current formulation of SFHS is to be used clinically, it will have to be administered continuously until blood is available for transfusion, and the patient's intravascular volume should be monitored carefully to prevent hypovolemia.

ABSTRACT

Retinal morphology serves as an extremely sensitive endpoint to hypoxic and ischemic conditions manifested by circulatory perturbations. Therefore, the effect of massive transfusion of stroma-free hemoglobin solution (SFHS) on retinal morphology of rats was evaluated. Seventy- three rats were divided into three groups. Two groups were transfused to 75% blood volume replacement-- one (n = 30) with 7% SFHS; one (n = 26) with 7% albumin solution; and the third group (n = 17) was cannulated, not transfused (controls). Animals in each group were killed at 1, 5, 12, 24 hr and 2 mo after the procedure. In the transfused rats, focal and perivascular regions of edema, axonal swelling, and vacuoles were observed by light and transmission electron microscopy in the nerve fiber layer of the central retina. These conditions progressively decreased from 1 to 12 hr in the albumin-treated group. The retinas of SFHS-treated rats killed at 12 and 24 hr had similar but more severe morphologic changes than any of the albumin-treated animals; swelling was more severe in those retinas obtained at 24 than at 12 hr, while vacuoles were larger in animals obtained at 12 hr. Abnormalities were observed in the prelaminar portion of the optic disc of the SFHS-treated groups killed at 12 and 24 hr. Subretinal hemorrhaging occurred in about 50% of the SFHS-treated animals killed at both 12 and 24 hr and was associated with swelling, vacuolization, and disruption of the photoreceptor outer segments and retinal pigment epithelium. Below normal levels of glycogen were present in the Müller cells of the retinas of albumin-treated rats killed at 5, 12, and 24 hr. At 12 hr after transfusion the Müller cells in lesions of the retinas obtained from the SFHS-treated rats were devoid of glycogen. High glycogen levels, however, appeared in a zone peripheral to the lesions. The latter effect was not apparent in the specimens obtained at 24 hr. The damage observed was probably due to hypoxic and ischemic effects secondary to urinary hemoglobin excretion and concomitant blood volume loss. No abnormalities were seen in the controls. The retinas of SFHS-treated rats killed at 1 and 5 hr showed normal retinal morphology and glycogen levels. Presumably, SFHS exerted a protective effect during this time period. If the current formulation of SFHS is to be used clinically, it will have to be administered continuously until blood is available for transfusion, and the patient's intravascular volume should be monitored carefully to prevent hypovolemia.

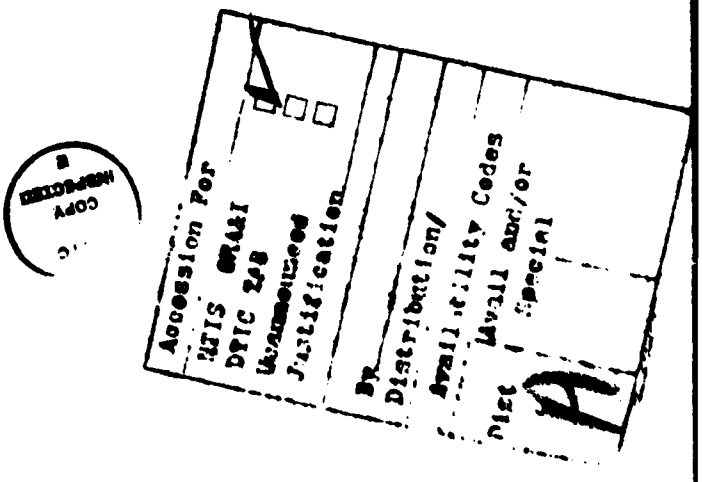

PREFACE

We wish to thank Toichiro Kuwabara, M.D., for his stimulating conversations and constructive comments; Thomas H. Hironaga, Angelo I. Zegna, and Kenneth R. Busse for their technical assistance; Richard Wheeler for assistance with photography; John P. Hannon, Ph.D., for review of the manuscript; Lottie B. Applewhite, M.S., for editorial assistance and assembly of the report; and Ann L. Wilkinson for preparation of the narrative typescript in the body of the report.

A shorter version of this report has been accepted for publication by the journal, Laboratory Investigation.

Harold I. Friedman, M.D., Ph.D., formerly a member of the staff at Letterman Army Institute of Research, is affiliated with the Department of Surgery, University of Arizona, Health Services Center, Tucson, Arizona.

TABLE OF CONTENTS

Over the past several decades both civilian and military researchers have been interested in the development of asanguinous fluid solutions for use in acute resuscitation from hypovolemic shock. Currently employed solutions, which include lactated Ringer's solution, plasmanate and salt-poor albumin, are capable of restoring intravascular volume, but they all lack the critical ability to transport and off-load oxygen to tissues. These properties naturally reside within red blood cells in the hemoglobin molecule; therefore, investigative efforts have been turned toward the formulation of a resuscitative solution containing hemoglobin. During early studies (1-4), when free hemoglobin was injected into laboratory animals and man, it caused adverse renal side effects. Later, these side effects were attributed to red blood cell stromal contaminants (5,6) and not to the hemoglobin molecule. This finding led DeVenuto et al (7) to develop a hemoglobin solution free of stromal contamination for use in acute resuscitation.

Although the physiological and biochemical properties of stroma-free hemoglobin solution (SFHS) have been extensively studied in laboratory animals (5,6,8-13), there is a paucity of information regarding the morphological consequences of administering massive quantities of SFHS to animals. Furthermore, there has been little documentation of the effects of SFHS on the central nervous system.

The retina provides a sensitive end-point for the morphological expression of focal and/or generalized ischemia, hypoxia, or focal vascular insufficiency because of its microcirculatory anatomy. The central retinal artery supplies the inner two-thirds of the retina while the remaining one-third, which has no vessels at all, is supplied by the choriocapillaris circulation (14-17). Examples of retinal response to perturbations in the vascular supply include cotton-wool spots (18-20), axonal swelling and cytoid body formation (16-18), intraretinal hemorrhage (16), and edema and vacuolization of the nerve fiber and ganglion cell layers as a result of retinal ischemia (18-21). Thus, retinal morphology serves to correlate changes which may be due to hypovolemia resulting in circulatory insufficiency and ischemia or temporary hypoxia. Using retinal histology and ultrastructural techniques, we compared the effects of massive exchange transfusion of SFHS on the rat retina with the

effects of exchange transfusing an albumin solution which commonly is infused in acute resuscitation.

MATERIALS AND METHODS

Seventy-three Sprague Dawley rats (200-250 g each) were fasted for 24 hr and divided into three experimental groups. Animals in group I were anesthetized with ether and underwent 75% blood volume exchange with a 7 g/dl solution of SFHS. The latter was prepared from outdated bank blood by using a previously described crystallization procedure (7). Exchange transfusion was performed at the rate of 1 ml per minute through a cannula inserted in the internal jugular vein. The transfusion was continued until the hematocrit reached 25% of the initial pre-transfusion hematocrit. Animals in group II were similarly exchange transfused with a 7 g/dl albumin solution, while rats in group III underwent cannulation, but did not receive an exchange transfusion.

After a scheduled time interval (Table 1), animals were reanesthetized, both eyes were enucleated and placed in a cold (4 C) fixative (3% glutaraldehyde-2% paraformaldehyde) (22) in 0.1 M phosphate buffer, pH 7.3, then the animals were euthanized (T-61, Euthansia Solution, Nat. Lab. Corp., Somerville, NJ). Subsequently, the globes were punctured with a sharp scalpel at the limboscleral margin and reimmersed into fixative. After 1 minute, the globe was divided into posterior and anterior poles. The posterior cup was further dissected into a 2-mm strip which included the optic nerve in the center. The retinal tissue was prepared for electron microscopy according to a previously described technique (23). Briefly, the tissue was post-fixed in phosphate-buffered 1% OsO_4, dehydrated in ethanol, and embedded in a 1:1 molar ratio of Epon 812 and Araldite 6005. Thick sections (0.5 to 1.0 um) for light microscopy were stained with methylene blue-azure II and 0.02% aqueous basic fuchsin (24). Cross-sections including the optic nerve and lesions were selected for ultramicrotomy. Thin sections, doubly stained with 2% uranyl acetate (25) and lead citrate (26), were observed with a Hitachi HS-8F-2 electron microscope. Slight, moderate, and severe degrees of pathologic change were subjectively determined for all the specimens evaluated (Table 1).

In addition, after fixation, representative retinal specimens were embedded in glycol methacrylate and stained with periodic acid-Schiff. Control sections were treated with α amylase (1,4-α-D-Glucan 4-glucanohydrolase; Sigma Chemical Co.,St.Louis, MO) then followed by periodic acid-Schiff (21).

RESULTS

All animals, up to 5 hr after transfusion with either 7% albumin or 7%

Table 1. Summary of number of animals evidencing changes in retinal morphology.

Treatment Groups	Rat Survival Times After Transfusion or Cannulation				
	1 Hr	5 Hr	12 Hr	24 Hr	2 Mo
I. 7% SFHS[a]					
No. of animals killed	7	6	5	7	5
(Total = 30)					
Degrees of pathologic change[b]			S,M,Sl	S,M,Sl	
No. of animals evidencing:					
Hemorrhage			3,0,0	4,0,0	
Vacuoles			4,0,1	0,4,3	
Swelling			1,3,1	4,1,2	
II. 7% Albumin[a]					
No. of animals killed (Total = 26)	7	5	5	4	5
Degrees of pathologic change[b]	S,M,Sl	S,M,Sl	S,M,Sl		
No. of animals evidencing:					
Hemorrhage					
Vacuoles	0,1,3	0,0,2	0,0,1		
Swelling	0,0,3	0,0,2	0,0,1		
III. Controls[c]					
No. of animals killed	3	3	3	3	5
(Total = 17)					

[a]These groups received an approximate 75% blood volume replacement with the solution indicated. [b]Sl = slight; M = moderate; S = severe. Severe degrees of hemorrhage, vacuolization, and swelling are represented in Figures 1, 2, and 6, respectively. [c]All controls received anesthesia and cannulation but no transfusion.

No entry or 0 = no changes in retinal morphology.

SFHS, showed decreased activity and alertness. By 12 hr, the animals in both groups were less languid, and by 24 hr they were still less active than the control animals. At 2 mo, all animals appeared physically normal.

Light Microscopy. All of the control animals, and albumin-transfused animals killed at 24 hr and 2 mo had normal-appearing retinas (Figure 1). Similarly, animals given SFHS and then killed 1, 5 hr, and 2 mo later also displayed normal retinal morphology. One, five, and twelve hours after albumin transfusion, retinas showed a subtle edematous swelling of the nerve fiber layer. This change was most evident in the retinas of the group killed 1 hr after transfusion, and only slightly apparent in the group killed at 12 hr. However, 12 hr after exchange transfusion with SFHS, focal zones in the central fundus frequently exhibited large oval-shaped vacuoles in the perivascular area of veins (Figure 2) and arteries (Figure 3) of the inner retina. The prelaminar portion of the optic disc (Figure 4) and the optic nerve (Figure 5) also contained these vacuoles. The largest vacuoles occurred in retinas obtained 12 hr after SFHS treatment. Retinas 24 hr after SFHS treatment showed an increased number of smaller vacuoles; these usually extended deeper into the outer retina (Figure 6). Many of these vacuoles contained a dense staining material and often extensive vacuolization produced localized bulges in the inner limiting membrane or the disc surface. Cells of the inner retina that were situated several microns lateral to the large vacuoles showed few changes. Ganglion cells, however, in the region of vacuolization usually exhibited swollen nuclei and lightly stained axoplasm (Figure 2).

Swelling of the inner retinal layers was mostly confined to localized regions around vessels (arteries and veins) in animals killed at 12 and 24 hr after SFHS treatment. In vessel-free regions, normal inner retina was commonly observed adjacent to affected areas. Affected areas were characterized by a focal but uniformly pale-staining cellular cytoplasm in the inner retina. Swelling appeared to increase in the retinas of SFHS-treated animals killed 24 hr after exchange transfusion (Table 1).

Subtle degenerative changes that were not focally localized in the retina were present in both photoreceptor outer segments and in the retinal pigmented epithelium of rats killed 24 hr after SFHS treatment. These changes appeared to be more advanced in the central fundus (Figures 7-10).

With more severe lesions the full thickness of the retina was involved. In these cases, the retina was markedly vacuolated,

swollen, and often had focal areas of photoreceptor involvement (Figure 6) and retinal hemorrhage (Figures 11-13). Hemorrhage was grossly observed in more than 50% of the SFHS-treated animals killed at both 12 and 24 hr (Table 1), but was more prominent at 24 hr after exchange transfusion. The hemorrhage had a blot configuration ranging from 0.25 to 1.25 mm in diameter (Figures 11 and 12) and was an intraretinal type (Figure 13). Since no ophthalmoscopy was performed, the precise quadrant location of these hemorrhages is unknown. From eye-cup preparations, the distribution, however, appeared equal for both the central and peripheral fundus. The hemorrhage was associated with disruptions of the outer limiting membrane , thereby producing red-cell-filled spaces between the inner plexiform layer and the retinal pigmented epithelium. In addition, the hemorrhage was associated with vacuolization and disruption of the distal portion of photoreceptor outer segments (Figure 6). In other experiments, SFHS-treated rats at 6 hr after exchange transfusion demonstrated free hemoglobin values of only 1.6 to 1.8 g/100 ml and reduced platelet counts.

Only the retinas from SFHS-treated animals killed at 12 hr showed a pinkish stain of Müller cells in the region between the ganglion cell layer and inner limiting membrane when the tissue was stained with periodic acid-Schiff. Complementary control sections treated with diastase (αamylase) followed by periodic acid-Schiff showed no staining of the Müller cells in similar regions, and indicated the presence of α-amylase-labile glycogen. Controls and the remaining groups treated in a similar manner showed little distinguishable staining difference and, therefore, must have contained minute amounts of α-amylase-labile glycogen.

Electron Microscopy. Retinal ultrastructure appeared normal in control rats, in albumin-exchanged transfused animals killed at 24 hr and 2 mo, and in SFHS-treated rats killed at 1 and 5 hr, and 2 mo after transfusion (Figure 14). In contrast, individual nerve fibers, occasional Müller cell processes and the extracellular space demonstrated marked vacuolization 12 hr after exchange transfusion with SFHS (Figures 15 and 16). Greatly swollen axons with intact membranes appeared among normal and compressed axons (Figure 15). The swollen segments of both axons and Müller cells, which were characterized by a less dense cytoplasm, contained fine granular material, swollen mitochondria, microvesicles, microfilaments, tubules, and membranous whorls. Other Müller cells were characterized by swollen mitochondria and dense cytoplasm (Figure 15). Müller cells adjacent to large vacuoles appeared shrunken (Figure 16). This vacuolization was closely correlated with the vacuolization observed at the light microscope level. Ganglion cells in these regions also appeared abnormal, with heterochromatin clumping, swollen

mitochondria, free ribosomes, and a highly vacuolated endoplasmic reticulum (Figure 17). The axons and dendrites of the inner plexiform layer had smaller vacuoles and swollen mitochondria, and many small vesicles which may have been of endoplasmic reticulum origin (Figure 18). In severely vacuolated retinas myelinated axons of the optic nerve showed changes similar to the axons of the nerve fiber layer (Figure 19). The degree of vacuolization in some specimens diminished with increasing distance from the nerve fiber layer or from the focal lesion. In addition, the albumin-treated animals killed at 1,5, and 12 hr showed similar but much reduced extent of ultrastructural change in the retinas. These changes were most apparent in the animals killed at 1 hr and almost nonexistent in animals killed at 5 and 12 hr (Table 1).

Twenty-four hours after exchange transfusion with SFHS, the inner retinal vacuoles were smaller but they extended deeper and more laterally into the retina. These vacuoles were also filled with flocculent debris and microvesicles. Again, vacuolated axons were interspersed between axons of both normal and compressed diameter. The degree of inner retinal swelling, as evidenced by a less dense cellular cytoplasm, appeared greater in animals killed at 24 hr than at 12 hr after SFHS treatment (Table 1). Axons with a swollen axoplasm and sometimes disrupted axolemma contained microvesicular bodies and membranous whorls. A large number of ganglion cells were also in the swollen state, and many contained clumped nuclear chromatin and abnormally swollen organelles. The inner plexiform layer at 24 hr also appeared more swollen than the 12-hr specimen. An occasional macrophage containing dark-staining inclusion material was observed in the ganglion cell region. Many dense bodies composed of membrane whorl-like formations as well as swollen mitochondria and vesicles were present in the inner plexiform layer. In some specimens, prominent glial-like fibers were observed in the ganglion cell, inner plexiform, and inner nuclear layer regions at 24 hr. Where full-thickness involvement occurred, vacuoles and swelling were present throughout all layers as was the presence of the hemorrhage. Where subretinal hemorrhaging occurred, red blood cells and flocculent debris (presumably SFHS) separated the photoreceptor outer segments from the retinal pigmented epithelium (Figure 20). In these regions the photoreceptor outer segments were disarrayed (Figures 20 and 21) and the retinal pigmented epithelium demonstrated marked vesiculation and swelling of the microvilli and distention of the basal infoldings (Figure 22).

Alteration in the integrity of cell tight junctions of both the retinal pigmented epithelium (Figure 23) and endothelial cells in inner retinal vessels (Figure 24) implied points of breakdown of the blood-retinal barrier.

Retinas of control and transfused rats killed at 1 hr and 2 mo demonstrated normal glycogen distribution patterns in inner retinal Müller cells (Figure 25). The glycogen content of the Müller cells of the albumin-treated rats killed at 5 hr was less than the glycogen content of the SFHS-treated animals killed at 5 hr after transfusion. At 12 hr, however, the retinas of the SFHS-treated rats had focal areas at and near lesions which were completely devoid of glycogen particles (Figure 26). The periphery of the devoid regions often demonstrated an increase in glycogen content (Figure 27) and in part explained the increase in periodic acid-Schiff stain observed at light microscopy. Compared to the albumin group, the SFHS group killed at the same time (24 hr after transfusion) demonstrated a generalized decrease of retinal glycogen in Müller cells. Table 2 summarizes the relative glycogen content in inner retinal Müller cells as a function of survival time after treatment received.

DISCUSSION

Stroma-free hemoglobin solutions offer several potential advantages over conventional asanguinous fluids in the treatment of hypovolemic shock. The most important of these is the ability to transport and off-load oxygen to tissues. However, as demonstrated in the current investigation, free circulating hemoglobin also has one property which will necessitate certain modifications in the way it is used to treat hypovolemia. Normally, hemoglobin in the red blood cell exists as a tetramer having a molecular weight of approximately 68,000. When hemoglobin is removed from the red blood cell and placed within the intravascular space, it partially dissociates into dimers (27). A portion of these dimers is rapidly bound to serum hepatoglobin, hemopexin, and albumin and undergoes degradation in the reticuloendothelial system. The remaining dimers cross the glomerular basement membrane of the kidneys, enter the renal tubules (12,28-30), and are excreted into the urine (12,28,29). The presence of hemoglobin in the renal tubules, in turn, induces a diuresis (12). Thus, as a consequence of the above sequence of events, intravascular half-retention time of free hemoglobin is only approximately 3.5 hr (10). Friedman et al (12,23) have demonstrated that the diuresis associated with a 75% whole blood volume exchange-transfusion with SFHS results in a 43% reduction in intravascular volume six hours after the exchange transfusion. The loss of hemoglobin from the vascular compartment, therefore, produces a loss of oxygen-carrying capacity and a reduction in circulatory volume. Based on the previous observations, it is not unreasonable to postulate that the retinal abnormalities observed at 12 to 24 hr after exchange transfusion with SFHS are a consequence of hypovolemia, hypoxia, and ischemia.

Blood osmolarities and oxygen tensions during exchange transfusion

Table 2. Summary of inner retinal Müller cell glycogen content as a function of survival time after treatment in rats.

Survival Times	Relative Glycogen Content of Inner Retinal Müller Cells as a Function of Treatment[a]
1 Hr	Control = SFHS-treated = Albumin-treated
5 Hr	Control > SFHS-treated > Albumin-treated
12 Hr	SFHS-treated[b] > Control > Albumin-treated
24 Hr	Control > Albumin-treated > SFHS-treated
2 Mo	Control = SFHS-treated = Albumin-treated

[a]Glycogen content was determined by subjective observation based on glycogen granule density in electron micrographs. The glycogen granule densities of SFHS and albumin-treated animals were compared to glycogen densities of the control (Figure 25). [b]At the light microscope level, some of the specimens demonstrated an increase over controls in periodic acid-Schiff stain uptake. At the electron microscope level, focal regions of swelling and vacuolization were completely devoid of glycogen granules (Figure 26) while regions peripheral to the morphologically altered regions showed a marked increase in glycogen granules (Figure 27).

with SFHS have been previously measured and discussed (31) and are not as critical in producing morphologic changes as the hypovolemia that develops as the result of diuresis. The small rise observed in blood urea nitrogen unaccompanied by a rise in serum creatine (29) may also be explained by the hypovolemia.

The swelling and vacuolization seen in the SFHS-treated rats were confined primarily to the inner retina, thereby suggesting that an altered blood flow through the retinal vessels rather than the choroidal vessels was the contributing factor to the observed morphological alterations. Similar swelling and vacuolization of the nerve fiber layer have been demonstrated in studies of experimental retinal ischemia where focal circulatory failure occurred (19,20,32,33). The widening of the interaxonal spaces suggests the potential death of axons and the degeneration of ganglion cells may be the first change that occurs as a result of SFHS-treatment.

Axonal swelling and vacuolization have been attributed to an intracellular acidosis induced by vascular insufficiency (18). Acidosis was reported to reach a peak within 25 to 30 min after the onset of ischemia (18); subsequently, the entry of water into ischemic neurons is rapid. Massive retinal swelling has been reported to occur in pigs after 3 to 60 min (33) and in monkeys after 15 min of ischemia (34). The swelling and vacuolization demonstrated in retinas of hypovolemic SFHS-treated rats were consistent with these findings.

Axonal swelling has been reported to interrupt organelle transport (20), but no regions of organelle accumulation on the axon-hillock side of ganglion cells (32) were observed in the retinas of SFHS-treated animals. The reason for the lack of organelle accumulation is unclear. Perhaps a generalized systemic hypovolemia is not as effective in interrupting transport as is a more complete focal embolization. Axonal swelling and vacuolization were more prominent in regions where the nerve fiber layer was thicker. Since no cytoid bodies (17) were observed in the nerve fiber layer of the SFHS-treated rat retinas, it may be postulated that the ischemic changes occurring in the retinas at 12 and 24 hr after treatment with SFHS were reversible. Support for this contention is derived from the fact that retinas of SFHS-treated rats were normal two months after exchange transfusion.

Reduced hemoglobin and platelet values have been previously reported to be associated with retinal hemorrhages (17). The retinal hemorrhages observed in this study may involve similar mechanisms (16). In addition, since the retina has a higher tissue pressure than

most other tissues (14), one might speculate that the high tissue pressure in association with the reduced blood volume observed in SFHS-treated animals may further aggravate the ischemic changes.

Both albumin and SFHS-treated animals had normal cerebral cortex, cerebellum, and hypocampus at all time periods studied after exchange transfusion (35). No morphological damage to the blood-brain barrier occurred by either solution. Presumably, from the extensive inner retinal vacuolization in SFHS-treated animals, a breakdown in the blood-retinal barrier occurred. Preferential damage to the blood-retinal barrier and not to the blood-brain barrier may have been partially due to the shunting away of blood from non-vital organs such as the liver and intestine and directed to the brain. Perhaps, in acute ischemia, the retina is included in this scheme. Furthermore, morphologic alteration of both the photoreceptors and the retinal pigmented epithelium may be a consequence of both the ischemic effects and a breakdown of the blood-retinal barrier. The fact that the distal tips of photoreceptor outer segments have been altered suggests that some retinal pigmented epithelium factors (hydrolitic enzymes?) have influenced outer segment membrane integrity. The extent to which the blood-retinal barrier became permeable needs to be clarified by additional studies utilizing horseradish peroxidase.

The normal composition of extracellular fluid of the inner layers of the retina must be maintained by transport across retinal capillaries or by modification of the chemical composition of the adjacent vitreous (36). The distribution of solutes within and their removal from the retina is aided by bulk fluid movements within extracellular fluid channels and by facilitated or active transport of solutes across the membranes of supporting elements, such as the Müller cells (36). In producing increased amounts of fluid in the extracellular spaces and shrinkage of Müller cells, the following events may ensue: (a) ischemia may inhibit active transport and increase the accumulation of solutes in the extracellular fluid by breakdown in the blood-retinal barrier (36); (b) the extracellular fluid becomes hypertonic around the Muller cells; (c) shrinkage of the Müller cells results from efflux of their fluid into the extracellular space; and (d) the osmolarity and increased extracellular fluid volume produces swelling and vacuolization. The extensive swelling and vacuolization in the inner retinal cells of the SFHS-treated animals, presumably, are also due to similar events (36).

The Müller cells in the retinas of SFHS-treated rats showed less ultrastructural alteration within lesions than the other inner retinal cells (18,33,37). Probably the extensive arborizations of the Müller fibers and their ability to receive oxygen and nutrients from both the

choriocapillaris and the retinal vessels render the cells more resistant at focal sites of ischemia. In addition, further resistance to ischemia is provided by their ability to synthesize and store glycogen which is mobilized under hypoxic conditions (21,38-40).

Previous studies indicate that retinal glycogen exists in a dynamic state between glycogen synthesis and glucose utilization, thereby serving as an energy reserve (21,41) to meet metabolic demands. In a compensatory response to metabolic needs, retinal glycogen content can increase, but if metabolic limits are exceeded, cellular deficiencies manifest themselves first as a reduction in glycogen content, then impaired function (42), and finally in tissue damage. A reduction in glycogen content was demonstrated in the retinas of SFHS-treated rats sacrificed at 12 hr. In this group, zones of complete glycogen depletion may have represented focal areas of increased metabolic demands secondary to the diuretically induced hypovolemia, ischemia, and hypoxia. The periphery of these zones, where an increase in glycogen was observed, suggests a response to injury similar to what others have observed (33,38,40,43). The generalized glycogen depletion observed in the retinas of the SFHS-treated group killed at 24 hr may reflect a more advanced state of the same catabolic process. However, the reduced glycogen content of the retinas from the albumin-treated rats killed at 5 hr as compared to the normal levels of the SFHS-treated animals at the same period of time suggests that the latter were able to maintain a more normal retinal metabolism prior to the disappearance of hemoglobin from circulation.

The morphological alterations seen in the retinas of SFHS-exchanged rats correlate well with those reported in the liver following exchange transfusion with SFHS (23). In both cases, SFHS appeared to protect both the liver and the retina from early hypoxic alterations observed after exchange transfusing with albumin or lactated Ringer's solution, presumably by its ability to transport and off-load oxygen to tissues. However, at later periods of time after transfusion, as a result of rapid disappearance of hemoglobin from the vascular space and subsequent hypovolemia, focal areas of both liver (23) and retinal degeneration were noted. Both the retinal and hepatic alterations appear to be reversible, and the hepatic alterations can be prevented by bolus infusions of additional SFHS (44). It remains to be seen if the same is true for the retinal lesions observed in this study.

CONCLUSIONS

The retinal alterations observed in the current investigation are probably a result of diminishing concentrations of circulating hemoglobin and a reduced intravascular volume. The implication of

these findings is that if the current formulation of SFHS is to be used clinically, it will have to be administered continuously until blood is available for transfusion, and the patient's intravascular volume should be monitored carefully to prevent hypovolemia.

RECOMMENDATIONS

It is recommended that multiple transfusions with SFHS be evaluated in rat retinas to confirm, as in the rat liver, the prevention of the hypovolemic effects. Similar studies should be conducted using monkeys or pigs as their retinal structure is similar to that of humans. In addition, it would also be useful to evaluate the effects of hypovolemia and ischemia using horseradish peroxidase tracer as an indicator of points of breakdown in the blood-retinal barriers and as an indicator of the extent of recovery from hypovolemic effects.

REFERENCES

1. BAKER, S.B., and R.L.F. DAWES. Experimental hemaglobinuric nephrosis. J Pathol Bacteriol 87:49-56, 1964

2. BRANDT, J.L., N.R. FRANK, and H.C. LICHTMAN. The effect of hemoglobin solutions on renal functions in man. Blood 6:1152-1162, 1951

3. JAENIKE, J.R., and E.E. SCHNEEBERGER. The renal lesion associated with hemoglobinemia. I. Its production and functional evaluation in the rat. J Exp Med 123:523-535, 1966

4. JAENIKE, J.R., and E.E. SCHNEEBERGER. The renal lesions associated with hemoglobinemia. II. Its structural characteristics in the rat. J Exp Med 123:537-545, 1966

5. BIRNDORF, N.I., and H. LOPAS. Effect of red cell stroma-free hemoglobin solution on renal function in monkeys. J Appl Physiol 29:573-577, 1970

6. RABINER, S.F., and L. FRIEDMAN. The role of intravascular hemolysis and the reticuloendothelial system in the production of a hypercoagulable state. Br J Haematol 14:105-118, 1968

7. DEVENUTO, F., T.F. ZUCK, A.I. ZEGNA, and W.Y. MOORES. Characteristics of stroma-free hemoglobin prepared by crystallization. J Lab Clin Med 89:509-516, 1977

8. AMBERSON, W.R, J.E. JACOBS, and A. HISEY. Hemoglobin saline solution as a transfusion media. In: Blood Substitutes and Blood Transfusion, edited by S. Mudd and S. Thalmier. Springfield, Illinois: Charles C. Thomas, 1942. pp 159-169

9. BONHARD, K. Acute oxygen supply by infusion of hemoglobin solutions. Fed Proc 34:1466-1467, 1975

10. DEVENUTO, F., W.Y. MOORES, A.I. ZEGNA, and T.F. ZUCK. Total and partial blood exchange in the rat with hemoglobin prepared by crystallization. Transfusion 17:555-562, 1977

11. DEVENUTO, F., and A.I. ZEGNA. Plasma oncotic pressure during and after blood exchange with crystalline hemoglobin solution. Surg Gynecol Obstet 147:379-384, 1978

12. FRIEDMAN, H.I., F. DEVENUTO, L. LOLLINI, P. MELLICK, and T.F. ZUCK. Morphologic effects following massive exchange transfusion with a stroma-free hemoglobin solution. II. Kidney. Lab Invest 40:655-667, 1979

13. MOSS, G.S., R. DEWOSKIN, A.L. ROSEN, H. LEVINE, and C.K. PALANI. Transport of oxygen and carbon dioxide by hemoglobin-saline solution in the red-cell-free primate. Surg Gynecol Obstet 142:357-362, 1976

14. ANDERS, B. Ocular circulation. In: Adler's Physiology of the Eye, edited by R.A. Mosses. St. Louis: C.V. Mosby Co., 1975. pp 210-231

15. HAYREH, S.S. Blood supply of the optic nerve head and its role in optic atrophy, glaucoma, and oedema of the optic disc. Br J Ophthalmol 53:721-748, 1969

16. HOGAN, M.J., and L.E. ZIMMERMAN. Ophthalmic Pathology. An Atlas and Text. Philadelphia: W. B. Saunders Co., 1962. p 449

17. YANOFF, M., and B.S. FINE. Ocular Pathology. A Text and Atlas. New York: Harper & Row, 1975. pp 24, 394-407, 574-578

18. ASHTON, N. Pathophysiology of retinal cotton-wool spots. Br Med Bull 26:143-150, 1970

19. DOLLERY, C.T., P. HENKIND, J.W. PATTERSON, P.S. RAMALHO, and D.W. HILL. Focal retinal ischaemia I. Opthalmoscopic and circulatory changes in focal retinal ischaemia. Br J Ophthalmol 50:285-324, 1966

20. MCLEOD, D., J. MARSHALL, E.M. KOHNER, and A.C. BIRD. The role of axoplasmic transport in the pathogenesis of retinal cotton-wool spots. Br J Ophthalmol 61:177-191, 1977

21. KUWABARA, T. Some aspects of retinal metabolism revealed by nistochemistry: Müller cells in pathological condition. In: Biochemistry of the Retina, edited by C.N. Graymore. New York: Academic Press, 1965. pp 93-98

22. RASMUSSEN, K.E. Fixation in aldehydes. A study on the influence of the fixative, buffer and osmolarity upon the fixation of the rat retina. J Ultrastructure Res 46:87-102, 1974

23. FRIEDMAN, H.I., F. DEVENUTO, L. LOLLINI, P. MELLICK, and T.F. ZUCK. Morphological effects following massive exchange transfusions with a stroma-free hemoglobin solution. I. Liver. Lab Invest 39:167-177, 1978

24. HUMPHERY, C.D., and F.E. PITTMAN. A simple methylene blue-azure-II basic fuchsin stain for epoxy-embedded tissue sections. Stain Technol 49:9-14, 1974

25. WATSON, M.L. Staining of tissue sections for electron microscopy with heavy metals. J Biophys Biochem Cytol 4:475-478, 1958

26. REYNOLDS, E.S. The use of lead citrate of high pH as an electron opaque stain for electron microscopy. J Cell Biol 17:208-212, 1963

27. BUNN, H.F., and J.H. JANDL. Exchange of heme among hemoglobins and between hemoglobins and albumin. J Biol Chem 243:465-475, 1968

28. ERICSSON, J.L.E. Transport and digestion of hemoglobin in the proximal tubule. I. Light microscopy and cytochemistry of acid phosphatase. Lab Invest 14:1-15, 1965

29. ERICSSON, J.L.E. Transport and digestion of hemoglobin in the proximal tubule. II. Electron microscopy. Lab Invest 14:16-39, 1965

30. MILLER, F. Hemoglobin absorption of the cells of the proximal convoluted tubule in mouse kidney. J Biophys Biochem Cytol 8:689-718, 1960

31. DEVENUTO, F., H.I. FRIEDMAN, J.R. NEVILLE, and C.C. PECK. Appraisal of hemoglobin solution as a blood substitue. Surg Gynecol Obstet 199:417-436, 1979

32. LEVY, N.S. The effect of interruption of the short posterior ciliary arteries on slow axoplasmic transport and histology within the optic nerve of the rhesus monkey. Invest Ophthalmol 15:495-499, 1976

33. SHAKIB, M., and N. ASHTON. Focal retinal ischaemia II. Ultrastrucural changes in focal retinal ischaemia. Br J Ophthalmol 50:325-382, 1966

34. KLOTI, R. Experimental occlusion of retinal and ciliary vessels in owl monkeys. I. Technique and clinical observations of selective embolism of the central retinal artery system. Exp Eye Res 6:393-399, 1967

35. FRIEDMAN, H.I., F. DEVENUTO, T.F. ZUCK and others. Histologic and ultrastructural effects of stroma-free hemoglobin solutions in rat liver, kidney, and brain. Surg Forum 28:3-5, 1977

36. BITO, L.Z., and C.J. DEROUSSEAU. Transport functions of the blood-retinal barrier system and the microenvironment of the retina. In: The Blood-retinal Barriers, edited by J.G. Cunha-Vaz. pp 132-163, New York: Plenum Press, 1980.

37. JOHNSON, N.F., and W.S. FOULDS. The effect of total acute ischaemia on the structure of the rabbit retina. Exp Eye Res 27:45-59,1978

38. JOHNSON, N.F. Retinal glycogen content during ischaemia. Albrecht von Graefes, Arch Klin Exp Ophthal 203:271-282, 1977

39. KUWABARA, T., and D.G. COGAN. Retinal glycogen. Arch Ophthalmol 66:96-104, 1961

40. ANTAL, M. Ketamine-induced ultrastructural changes in retina. Albrecht V. Graefs, Arch Klin Exp Ophthalmol 210:43-53, 1979

41. GRAYMORE, C.N. Biochemistry of the retina. In: Biochemistry of the Eye, edited by C.N. Graymore. New York: Academic Press, 1979. pp 674-675

42. AMES, A., III, and B.S. GURIAN. Effects of glucose and oxygen deprivation on function of isolated mammalian retina. J Neurophysiol 26:617-634, 1963

43. WASSILEWA, P., O. HOCKWIN, and I. KORTE. Glycogen concentration changes in retina, vitreous body and other eye tissues caused by disturbances of blood circulation. Albrecht von Graefes, Arch Klin Exp Ophthalmol 199:115-120, 1976

44. DEVENUTO, F., H.I. FRIEDMAN, and P.W. MELLICK. Massive exchange transfusions with crystalline hemoglobin solution and subsequent replacement of hemoglobin and blood volume. Surg Gynecol Obstet 151:361-365, 1980

FIGURES

Detailed legends for each figure appears with the figure. The following information is provided for interpretation of ...

Figures 1 through 4, 6 through 10, and 13. Full-thickness light micrographs of rat retina.*† The layers are identified as follows:

1 = nerve fiber layer
2 = ganglion cell layer
3 = inner plexiform layer
4 = inner nuclear layer
5 = outer plexiform layer
6 = outer nuclear layer
7 = photoreceptor cells
8 = retinal pigment epithelium

All bars on the light micrographs = 10 μm

Figure 5. Light micrograph of optic nerve taken from same specimen as Figure 4.

Figure 11. Gross photograph of eye-cup preparation from rat 24 hr after 75% blood volume replacement with stoma-free hemoglobin solution (SFHS).

Figure 12. Higher magnification of hemorrhagic area in the rat retina 24 hr after 75% blood volume exchange transfusion with SFHS.

Figures 14 through 27. Electron micrographs of rat retina.*‡ Some of the electron micrographs are correlated with the light micrographs (Figures 1, 2, 5, and 13).

*Tissue prepared according to Friedman et al (23) with modifications applicable to the retina.

†Stained according to techniques described by Humphrey and Pittman (24).

‡Tissue doubly stained with 2% uranyl acetate (25) and lead citrate (26).

APPENDIX

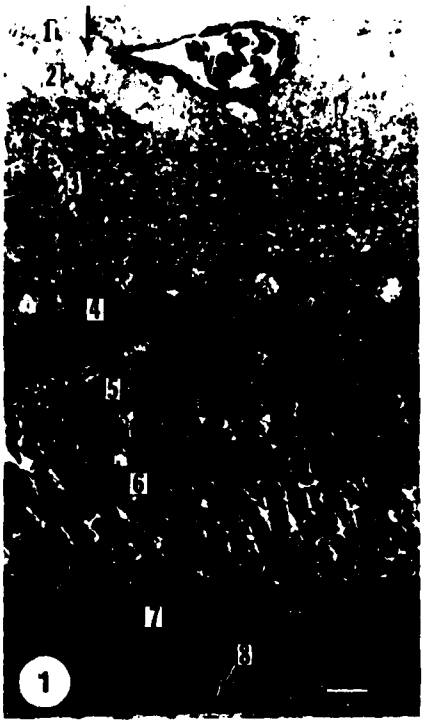

Figure 1. Control rat retina. All layers appear normal. Arrow indicates nerve bundle. Vein (v).

Figure 2. Rat retina 12 hr after 75% blood volume replacement with SFHS. Large vacuoles *(arrow)* surround a vein (v). The inner and outer plexiform layers (3 and 5, respectively) have a few small vacuoles. The photoreceptor (7) outer segments (os) are normal but have been artifactually detached from the pigment epithelium in this section.

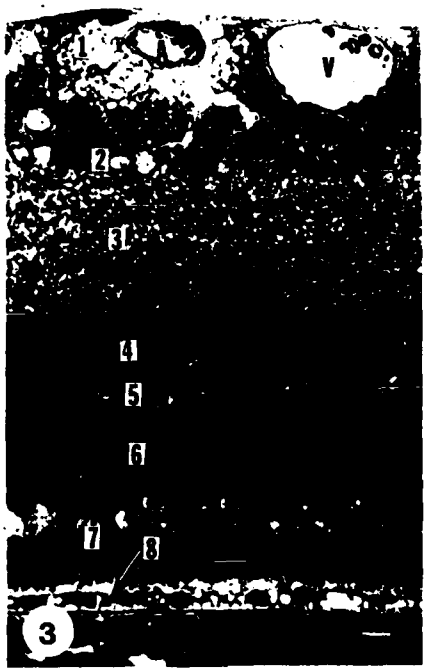

Figure 3. Rat retina 12 hr after 75% blood volume replacement with SFHS. An artery (**A**) is adjacent to a vein (**V**). Many vacuoles surround the artery. The inner and outer plexiform layers and the retinal pigment epithelium (3, 5, and 8, respectively) also contain many small vacuoles. The photoreceptor (7) outer segments appear normal.

Figure 4. Rat retina 12 hr after 75% blood volume replacement with SFHS. Meridional section through the prelaminar portion of the optic disc (**OD**). Nerve fiber bundles (1) coming from the retina show large vacuoles (*arrows*), some of which are adjacent to a branch from the central retinal vein (**V**). The adjacent inner and outer plexiform layers and retinal pigment epithelium (3, 5, and 8, respectively) are vacuolated. Photoreceptors (7) are normal.

Figure 5. Light micrograph of optic nerve taken from the same specimen as Figure 4 (tangential section). Many large vacuoles are present in the optic nerve tract *(arrow)*.

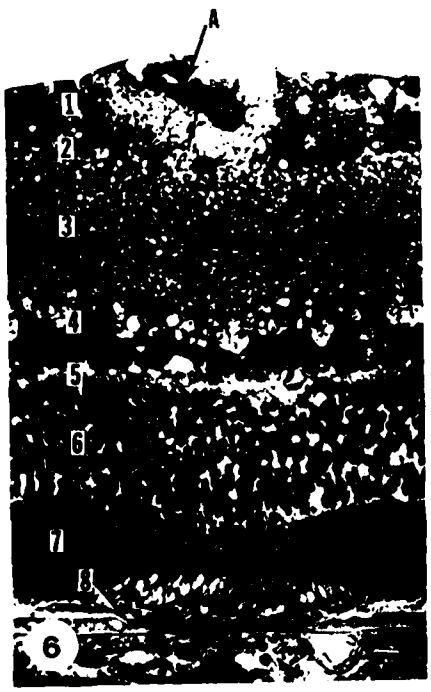

Figure 6. Rat retina 24 hr after 75% blood volume replacement with SFHS. Many vacuoles surround an artery (**A**). The swelling and vacuolization in the inner and outer plexiform layers (3 and 5, respectively) are similar to the findings in Figure 4. One exception, however, includes the vacuolization, disruption and dark staining of the photoreceptor (7) outer segments and the retinal pigment epithelium (8).

Figure 7 (left).* Light micrograph taken in the retinal periphery. Most of the photoreceptors (7) and RPE cells (8) are normal while many small vacuoles are present in the inner retinal layers (1 through 5). One RPE cell (*arrow*) stained dark. The photoreceptor outer segments are slanted; this is indicative of a more peripheral retinal location.

Figure 8 (right).* Light micrograph more central in retinal location than Figure 7. The inner retina (layers 1 through 5) is vacuolated and some of the photoreceptor (7) outer segments stained dark at their distal tips (*arrow*). The RPE (8) is normal. Note the slight separation between the photoreceptor outer segments and the RPE (compare with Figure 7).

*Same section rat retina 24 hr after 75% blood volume replacement with SFHS (Figures 7 through 10).

Figure 9 (left).* Light micrograph more central in retinal location than Figure 8. The photoreceptor (7) outer segments stained dark at their distal tips and some are vacuolated *(large arrow)*. Dark inclusion bodies *(small arrow)* are present in the RPE cells (8).

Figure 10 (right).* Light micrograph from the central retina. Both distal tips of the photoreceptor (7) outer segments and the RPE (8) stained dark. The dark stained areas represent degenerative changes. An inner retinal vessel (v), probably an artery, is collapsed. Many small vacuoles are present under this vessel in the inner plexiform layer (3). A more focal and more severe expression of these degenerative changes may be represented in Figure 6.

*Same section rat retina 24 hr after 75% blood volume replacement with SFHS (Figures 7 through 10).

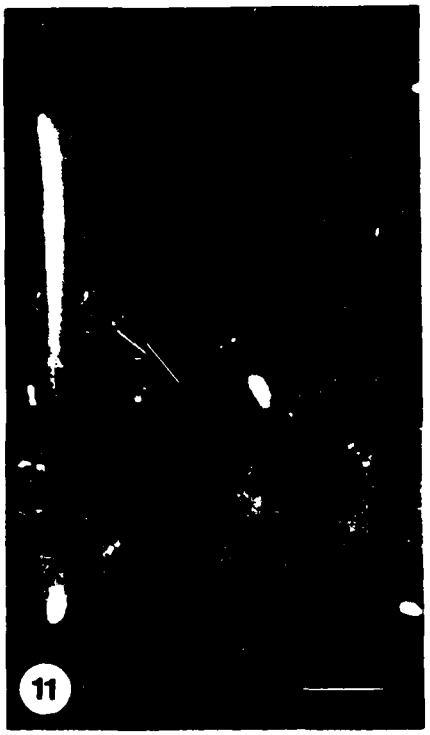

Figure 11 (left). Gross photograph of eye-cup preparation from rat 24 hr after 75% blood volume replacement with SFHS. Posterior pole shows many small hemorrhages *(arrow).*
Figure 12 (right). Higher magnification (than Figure 11) of hemorrhagic area. Hemorrhage shows radiating spokes *(arrow)* which are characteristic of subretinal hemorrhages. Central spot of hemorrhage is darker and out of focus, which suggests a locus higher in the inner retina.

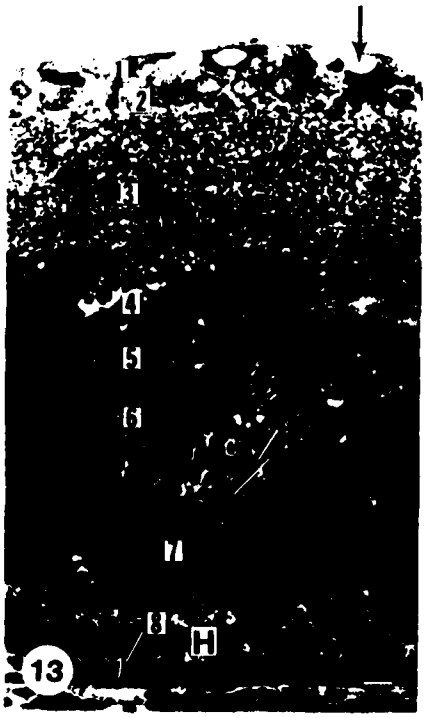

Figure 13 (left). Rat retina 24 hr after 75% blood volume replacement with SFHS. Cross-section through a focal hemorrhage. Red blood cells are present within most of the outer retinal layers and a large accumulation (H) occurred in the subretinal space. The source of hemorrhage is most likely an inner retinal vessel. There is a break in the outer limiting membrane *(large arrow).* The hemorrhage is relatively new because no hemosiderin deposits are apparent. Large vacuoles *(small arrow)* occurred in the nerve fiber layer (1). The inner plexiform layer (3) was moderately vacuolated. The inner nuclear layer (4), outer plexiform layer (5), outer nuclear layer (6), and photoreceptors (7) were highly disorganized and vacuolated.

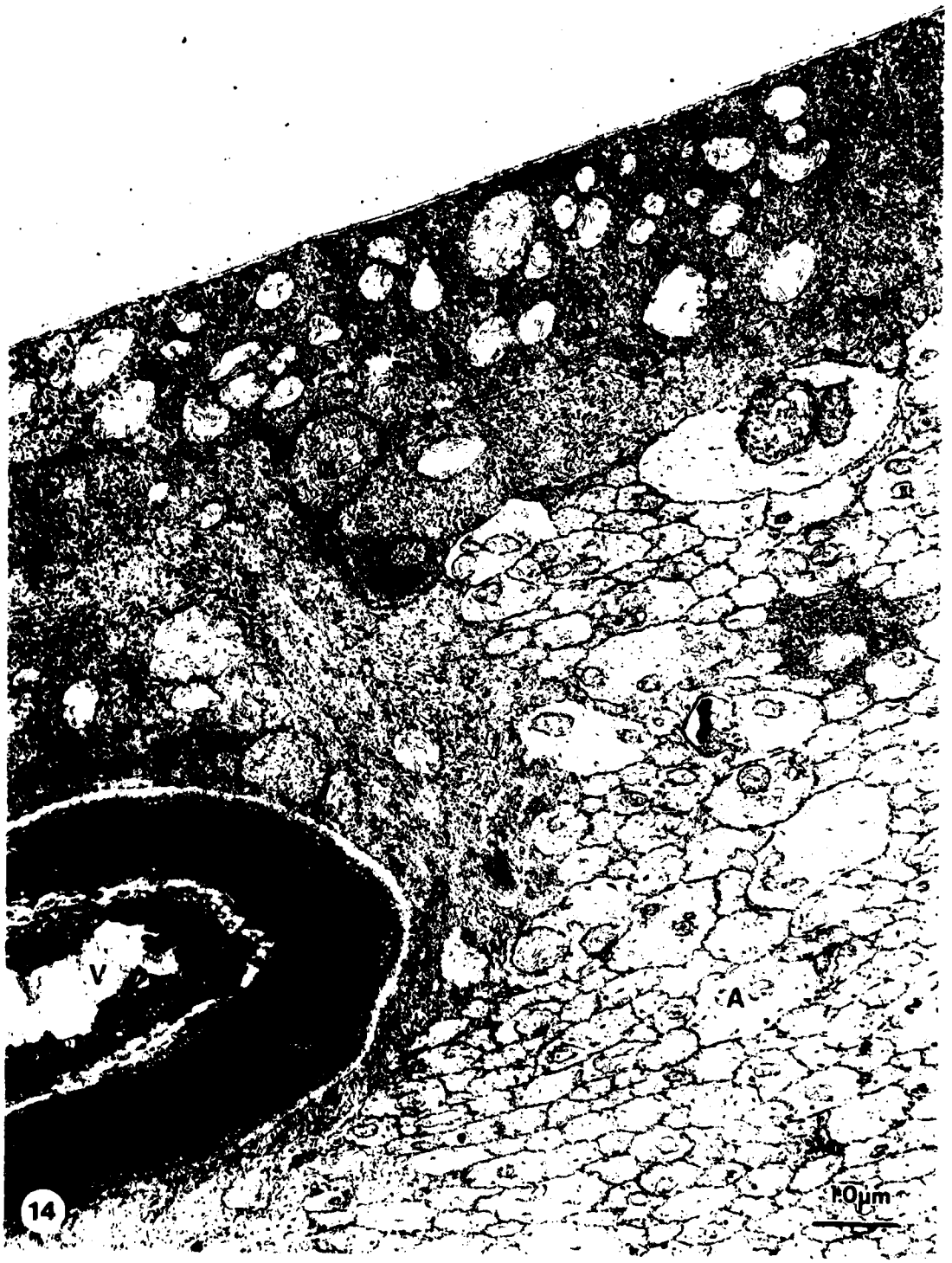

Figure 14. Electron micrograph of an area of retina from the control animal (Figure 1). Vein (**V**), axon (**A**), and mitochondria (**m**).

Figure 15. Electron micrograph of rat retina 12 hr after 75% blood volume replacement with SFHS. High magnification of specimen taken from same area as Figure 2. One Müller cell (M_1) stained dark and many of the mitochondria (m) are swollen and vacuolated. An adjacent Müller cell (M_2) is more normal in structure. A cross-section of an axon bundle (A), indicated by *large arrows*, contains some axons which are extremely swollen. ***Inset***, a longitudinal section through part of an axon bundle with focal swelling in an axon *(large arrow)*. Both swollen and normal appearing axons contain dense myelin forms *(small arrows)*.

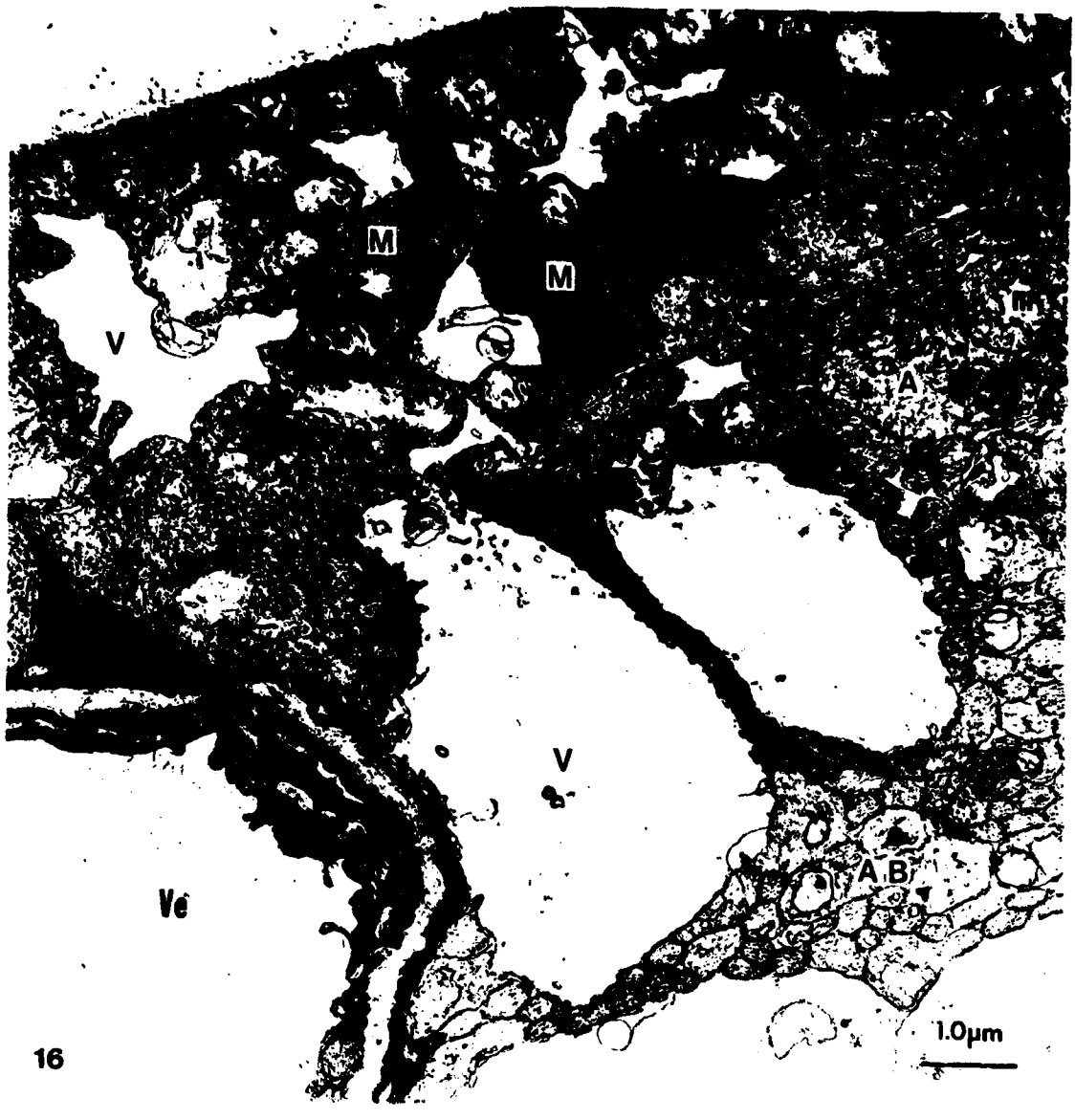

Figure 16. Electron micrograph of the rat retina (Figure 2) 12 hr after 75% blood volume replacement with SFHS. Large vacuoles (**V**) surround a retinal vein (**Ve**). The large vacuoles between an axon bundle (**AB**) and Müller cells (M_1 and M_2) represent areas of missing cellular constituents and a dilation of the extracellular space. Some axons (**A**) appear normal while others show swollen mitochondria (**m**).

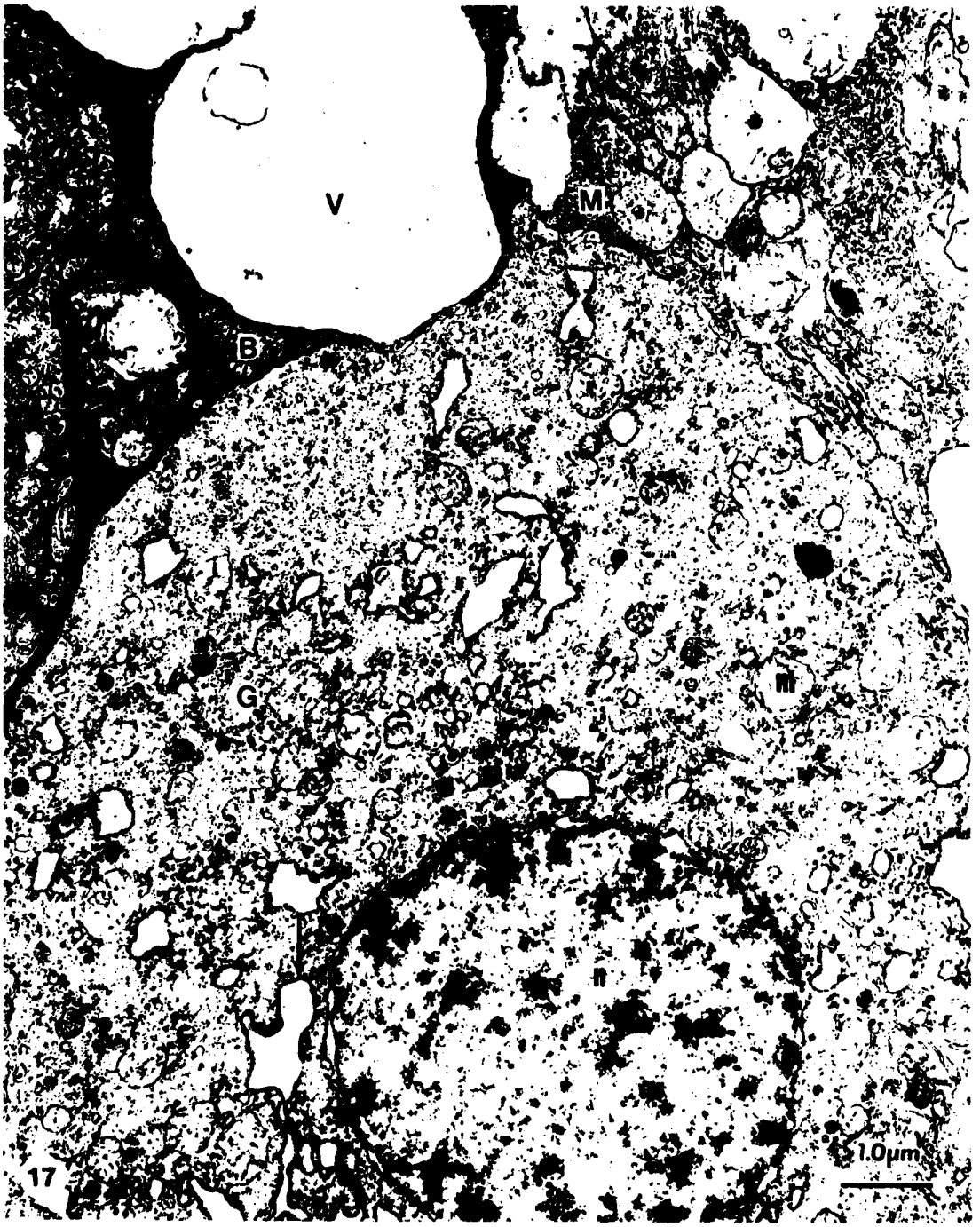

Figure 17. Electron micrograph of rat retina (Figure 2) 12 hr after 75% blood volume replacement with SFHS. A ganglion cell (**G**) with nucleus (**n**) shows a less dense cytoplasm, swollen mitochondria (**m**) and a markedly dilated endoplasmic reticulum (*arrow*). A large vacuole (**V**) is present adjacent to a nerve fiber bundle (**B**), a Müller cell (**M**) and a ganglion cell (**G**). Normal axons are present in the nerve fiber bundle.

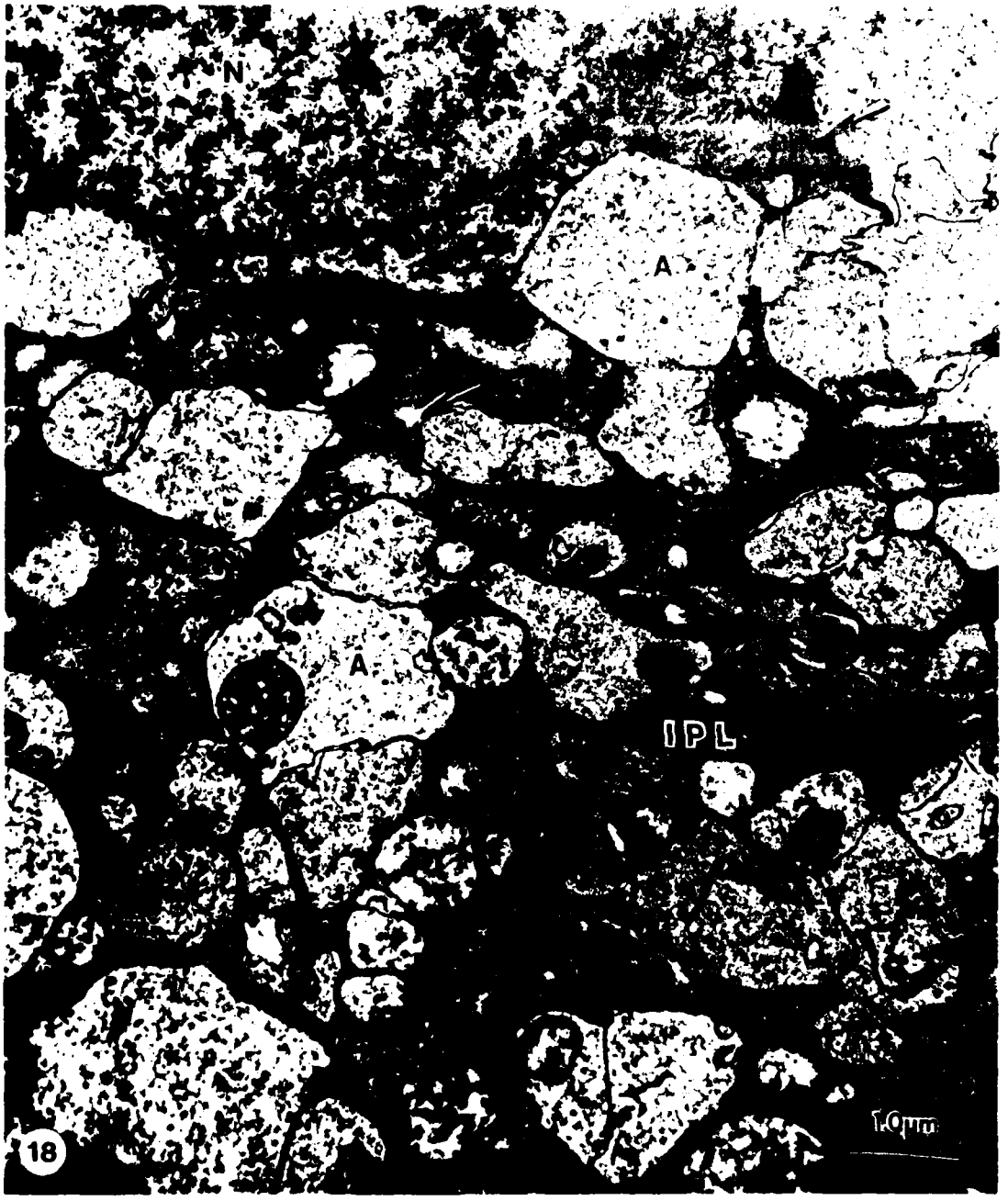

Figure 18. Electron micrograph of rat retina 12 hr after 75% blood volume replacement with SFHS. The inner plexiform layer (IPL) contained many swollen cellular processes, some of which may be axons (A). Many of the mitochondria (m) are also swollen. Cytoplasmic processes of the Müller cells are indicated by the arrows. Ganglion cell nucleus (N).

Figure 19. Transmission electron micrograph of rat optic nerve 12 hr after 75% blood volume replacement with SFHS. All photographs are taken from the same specimen as Figure 5.

Figure 19a (above). A myelinated axon (**A**) is filled with cellular debris and organelles. Small vacuoles (**V**) are present in this debris. The accumulation of cellular debris may reflect the interruption of axoplasmic transport processes. A core of neurofilaments (**N**) is present in the center. The myelin sheath of this axon shows focal points of degeneration (*arrows*). A more normal axonal segment is present at **B**. Dilation of extraaxonal areas (**E**) occurred between some axons.

Figure 19b (left). A myelinated axon (**A**) shows a more normal internal structure, however, degenerative myelin forms (**M**) are present in the cytoplasm and the myelin sheath shows focal points of breakdown (*arrows*).

Figure 19c (right). Large vacuoles in the optic nerve show no myelin sheath border and may be extraaxonal (**E**) while others show a complete myelin sheath border and are clearly intraaxonal (**A**).

Figure 20. Electron micrograph of rat retina 24 hr after 75% blood volume replacement with SFHS. Section taken from the same specimen as Figure 13. The subretinal hemorrhage is indicated by the red blood cells (**rbc**) present between the photoreceptor outer segments (**os**) and the retinal pigment epithelium (**R**). Some of the outer segments are pyknotic (*large arrow*) and the majority show a zone of alteration (*indicated by vertical bars*) at their distal tips. The inner segments (**IS**) appear normal. Dense filament-like bodies (*small arrows*) are also present in the subretinal space.

Figure 21 (left). Electron micrograph of rat retina 24 hr after 75% blood volume replacement with SFHS. Section taken from the same specimen as Figures 13 and 20. The retinal pigment epithelium (**R**) contains dense inclusion bodies, some of which are present outside the retinal pigment epithelium (*small arrow*). The dense filament-like bodies (**F**) are present at the apex of the microvilli (**mv**) and may be the result of recrystallized SFHS. The outer segments (**OS**) are both vacuolated and pyknotic (*large arrow*). Red blood cell (**rbc**).

Figure 22 (right). Electron micrograph of rat retina 24 hr after 75% blood volume replacement with SFHS. Section taken from same specimen as Figures 13, 20, and 21. The retinal pigment epithelium (**R**) shows swollen basal infoldings (*large arrow*). Many of the apical microvilli (*small arrows*) are also swollen and surrounded by dense flocculent material. Dense filament-like bodies (**F**) are present in the subretinal space. Red blood cell (**rbc**).

Figure 23 (left). Electron micrograph of rat retina 24 hr after 75% blood volume replacement with SFHS. High magnification of retinal pigment epithelium apex of Figure 22. Arrow indicates cell-tight junction. The extracellular space (S) between retinal pigment epithelial cells is swollen and may represent a breakdown of the blood-retinal barrier. Mitochondria (m).

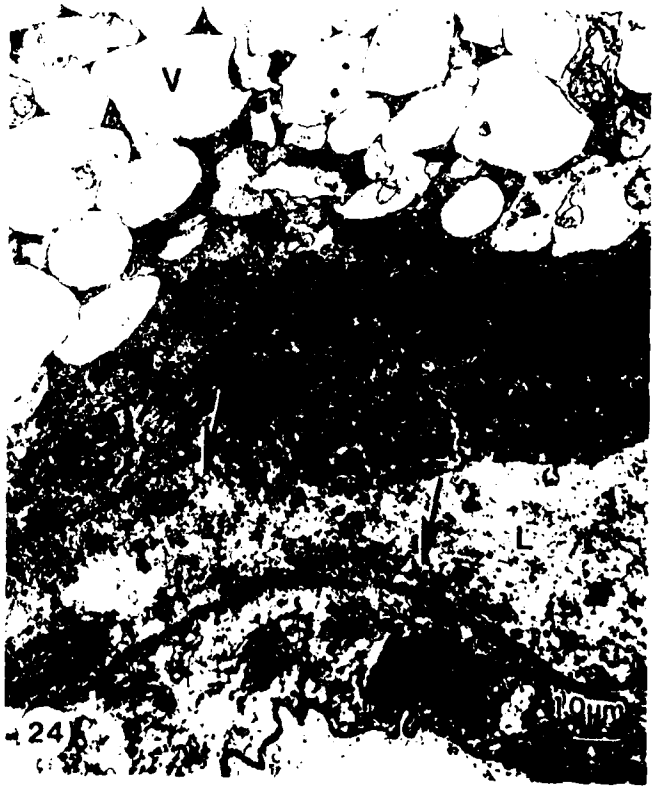

Figure 24 (right). Electron micrograph of rat retina 24 hr after 75% blood volume replacement with SFHS. Lumen (L) of inner retinal vein contains debris. Endothelial cell integrity is disrupted (*large arrows*) indicating the breakdown of the blood-retinal barrier in the inner retina. Vacuoles (V) are present in the adjacent nerve-fiber layer.

Figure 25 (opposite page). High magnification electron micrograph of retina from a control animal. A diffuse scattering of small glycogen particles (*arrows*) are present in the Müller cell cytoplasm. Mitochondria (**m**).

Figure 26 (opposite page). High magnification electron micrograph of rat retina 12 hr after 75% blood volume replacement with SFHS in the region of vacuolization (Figure 2). The extracellular space (**ECS**). is highly dilated between Müller cells M_1 and M_2. Arrow indicates cell borders. Mitochondrial cristae are severely disarranged and Müller cell cytoplasm is devoid of glycogen particles.

Figure 27 (opposite page). High magnification electron micrograph of rat retina 12 hr after 75% blood volume replacement with SFHS . It depicts the periphery of the zone of vacuolization (Figures 2 and 26). Large pockets of glycogen accumulation (*arrows)* are present in the Müller cells. At light microscopy, some of these regions showed a positive PAS stain for labile glycogen. Mitochondria (**m**) are swollen and contain disorganized cristae.

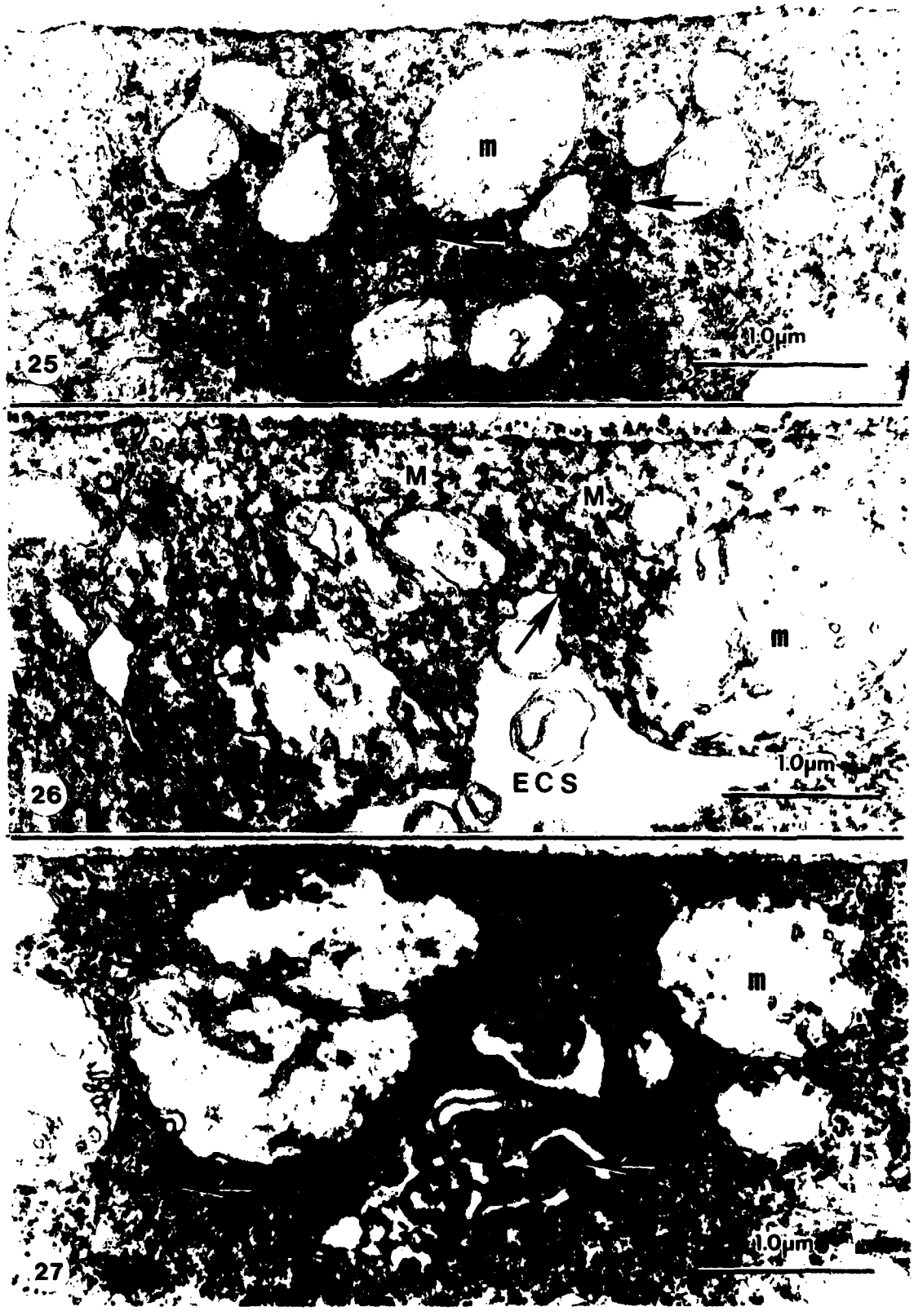
m
1.0μm
25
M
M
m
ECS
1.0μm
26
m
1.0μm
27

OFFICIAL DISTRIBUTION LIST

Commander
US Army Medical Research
and Development Command
ATTN: SGRD-RMS/Mrs. Madigan
Fort Detrick, Frederick MD 21701

Defense Technical Information Center
ATTN: DTIC-DDA (12 copies)
Cameron Station
Alexandria VA 22314

Director of Defense Research and Engineering
ATTN: Assistant Director, Environmental
and Life Sciences
Washington DC 20301

The Surgeon General
ATTN: DASG-TLO
Washington DC 20314

HQ DA (DASG-ZXA)
WASH DC 20310

Commandant
Academy of Health Sciences
ATTN: HSHA-CDM
Fort Sam Houston TX 78234

Assistant Dean
Institute and Research Support
Uniformed Services University
of Health Sciences
6917 Arlington Road
Bethesda MD 20014

Commander
US Army Environmental Hygiene Agency
Aberdeen Proving Ground MD 21070

US Army Research Office
ATTN: Chemical and Biological Sciences
Division
P.O. Box 1221
Research Triangle Park NC 27709

Biological Sciences Division
Office of Naval Research
Arlington VA 22217

Director of Life Sciences
USAF Office of Scientific Research (AFSC)
Bolling AFB
Washington DC 20332

Director
Walter Reed Army Institute of Research
Washington DC 20012

Commander
US Army Medical Research Institute
of Infectious Diseases
Fort Detrick, Frederick MD 21701

Commander
US Army Research Institute
of Environmental Medicine
Natick MA 01760

Commander
US Army Institute of Surgical Research
Brooke Army Medical Center
Fort Sam Houston TX 78234

Commander
US Army Medical Bioengineering
Research and Development Laboratory
Fort Detrick, Frederick MD 21701

Commander
US Army Aeromedical Research Laboratory
Fort Rucker AL 36362

Commander
US Army Research Institute
of Chemical Defense
Aberdeen Proving Ground
Edgewood Arsenal MD 21010

Commander
Naval Medical Research Institute
National Naval Medical Center
Bethesda MD 20014

Commander
USAF School of Aerospace Medicine
Aerospace Medical Division
Brooks Air Force Base TX 78235

END

FILMED

3-83

DTIC